

2 **Co-variation of crenarchaeol and branched GDGTs in globally-distributed**
3 **marine and freshwater sedimentary archives**

4 Susanne Fietz^{*a}, Carme Huguet^a, James Bendle^b, Marina Escala^{a,1}, Christopher
5 Gallacher^b, Lydie Herfort^{c,2}, Robert Jamieson^b, Alfredo Martínez-García^{a,3}, Erin L.
6 McClymont^{d,4}, Vicky L. Peck^e, Fredrick G. Prahl^f, Sergio Rossi^a, Gemma Rueda^a, Anna
7 Sanson-Barrera^a, Antoni Rosell-Melé^{a,g}

8 ^aICTA, Universitat Autònoma de Barcelona, 08193 Cerdanyola del Vallès, Spain

9 ^bGlasgow Molecular Organic Geochemistry Laboratory, University of Glasgow, Glasgow, G12 8QQ,
10 UK.

11 ^cDepartment of Marine Organic Biogeochemistry, Royal Netherlands Institute for Sea Research (NIOZ),
12 1790, Den Burg, The Netherlands.

13 ^dSchool of Geography, Politics & Sociology, Newcastle University, Newcastle upon Tyne, NE1 7RU, UK

14 ^eBritish Antarctic Survey, Cambridge, CB3 0ET, UK

15 ^fCollege of Oceanic & Atmospheric Sciences, Oregon State University, Corvallis, OR 97331-5503, USA

16 ^gICREA, Passeig Lluís Companys, 08010 Barcelona, Catalonia, Spain

17 ¹present address: Institute of Natural Resource Sciences, Zurich University of Applied Sciences,
18 Switzerland

19 ²present address: Center for Coastal Margin Observation & Prediction, Oregon Health and Science
20 University, Portland, Oregon, USA

21 ³present address: Eidgenössische Technische Hochschule (ETH) Zürich, Switzerland

22 ⁴present address: Department of Geography, Durham University, Durham DH1 3LE, UK.

23 ^{*}Corresponding author: Susanne Fietz, Institut de Ciència i Tecnologia Ambientals (ICTA), Universitat
24 Autònoma de Barcelona (UAB), Campus UAB, 08193 Cerdanyola del Vallès, Catalonia, Spain, Tel.: +34
25 93 581 4219, Fax: +34 93 581 3331, email: susanne.fietz@uab.cat, alternative email: s_fietz@web.de

26 e-mail-address of the co-authors:

27 Carme Huguet: Carme.Huguet@uab.cat

28 James Bendle: james.bendle@ges.gla.ac.uk

29 Marina Escala: marina.escala@zhaw.ch

30 Christopher.gallacher: Christopher.gallacher@glasgow.ac.uk

31 Lydie Herfort: herfortl@ebs.ogi.edu

32 Alfredo Martínez-García: alfredo.martinez-garcia@erdw.ethz.ch

33 Erin McClymont: erin.mcclymont@durham.ac.uk

34 Vicky Peck: vlp@bas.ac.uk

35 Fred Prahl: fprahl@coas.oregonstate.edu

36 Sergio Rossi: Sergio.Rossi@uab.cat

37 Gemma Rueda: gemma.rueda@uab.cat

38 Anna Sanson-Barrera: Anna.Barrera@uab.cat

39 Antoni Rosell-Melé: antoni.rosell@uab.cat

40

41 **ABSTRACT**

42 Two major types of glycerol dialkyl glycerol tetraethers (GDGTs) are commonly
43 used in paleoecological and paleoclimatological reconstructions: isoprenoidal and
44 branched GDGTs. In aquatic environments it was originally assumed that isoprenoidal
45 GDGTs, especially crenarchaeol, derive mainly from aquatic Thaumarchaeota, whilst
46 branched GDGTs are an allochthonous input derived from soil Bacteria. Recently,
47 direct co-variation of crenarchaeol and branched GDGTs has been described in two
48 marine sedimentary records, and this observation suggests *in situ* production of
49 branched GDGTs is possible at least in some aquatic environments. After investigating
50 30 published and unpublished data sets from downcore and surface sediments as well as
51 sediment traps from 15 distinct regions around the world we found a widespread
52 significant correlation between concentrations of branched GDGTs and crenarchaeol
53 ($p < 0.01$; $r^2 = 0.57-0.99$), even when normalized against TOC, where available. These
54 data sets include freshwater and marine environments with varying distances from the
55 shore, varying redox conditions and different terrestrial matter input pathways. Our
56 findings from this large-scale data set suggest that a common or mixed source for both
57 GDGT types is actually commonplace in lacustrine and marine settings.

58

59 **Keywords:** Archaea; branched GDGTs; crenarchaeol; *in situ* production; isoprenoid
60 GDGTs; lakes; oceans

61

62

1. INTRODUCTION

63 The glycerol dialkyl glycerol tetraethers (GDGTs) are cell membrane lipids of
64 Archaea and Bacteria that are used in paleolimnology and paleoceanography to track
65 changes in archaeal abundance, terrestrial organic matter input into aquatic systems and
66 to estimate past water and air temperatures. The two major types of GDGTs currently
67 used have isoprenoidal and branched structures.

68 Mesophilic Archaea synthesize isoprenoidal GDGTs and the isoprenoidal GDGT
69 crenarchaeol, for example, has become a marker for Thaumarchaeota (Sinninghe
70 Damsté et al., 2002). Thaumarchaeota, formerly known as Crenarchaeota group I
71 (Brochier-Armanet et al., 2008), are ubiquitously distributed in marine environments
72 (Fuhrman et al., 1992; DeLong et al., 1998; Massana et al., 2000) as well as in lakes
73 (Schleper et al., 1997; Keough et al., 2003; Casamayor and Borrego, 2009).
74 Consequently, isoprenoidal GDGTs and especially crenarchaeol, have been found
75 globally in marine and lacustrine water column and sediment samples (Powers et al.,
76 2010; Kim et al., 2010).

77 The branched GDGTs have been predominantly found in terrestrial settings such as
78 peat bogs and soils (Weijers et al., 2006a), but also in sedimentary settings receiving
79 significant terrestrial input (Hopmans et al., 2004). The glycerol stereochemistry of the
80 branched GDGTs supports a bacterial provenance (Weijers et al., 2006b) and recently a
81 branched GDGT could be identified in two cultures of Acidobacteria (Sinninghe
82 Damsté et al., 2011). However, these Bacteria are aerobes and the highest branched
83 GDGT concentrations are found in low-oxygen environments, suggesting that the
84 branched GDGTs are likely synthesized by other groups of Bacteria as well (Sinninghe-
85 Damsté et al., 2011).

86 Three main indices have been proposed for paleo-reconstructions in marine and
87 lacustrine sedimentary records using isoprenoidal and branched GDGTs, which are the
88 TEX₈₆ (Schouten et al., 2002), the MBT/CBT (Weijers et al., 2007) and the BIT
89 (Hopmans et al., 2004). The basic premise for those indices is that isoprenoidal GDGTs
90 are of aquatic origin and that the branched GDGTs are exclusively terrestrially-derived
91 and transported to the aquatic environment through erosion, rivers, ice rafting, etc.
92 However, isoprenoidal GDGTs including crenarchaeol have also been found in
93 terrestrial environments, e.g., in peat bogs and soils (Gattinger et al., 2003; Leininger et
94 al., 2006; Weijers et al., 2006a). Furthermore, a mixed allochthonous and autochthonous
95 source for branched GDGTs has been recently suggested in lakes (Sinninghe Damsté et
96 al., 2009; Bechtel et al., 2010; Blaga et al., 2010; Tierney et al., 2010; Zink et al., 2010;
97 Sun et al., 2011). Peterse et al. (2009) and Zhu et al. (2011) also proposed an
98 autochthonous source for branched GDGTs in marine coastal sites. In contrast,
99 Yamamoto et al. (2008) suggested an allochthonous source for crenarchaeol in the
100 central Arctic Ocean. Yamamoto et al. (2008) and Zhu et al. (2011) based their
101 conclusions on the strong correlation they observed between branched GDGT and
102 crenarchaeol concentrations.

103 In the present study, we show the pervasive significant correlation between branched
104 GDGTs and crenarchaeol in a wide range of aquatic environments. These include
105 sediment trap samples, surface sediments and downcore records from lacustrine and
106 marine settings. The sites were not initially selected for the purpose discussed here and
107 several data sets used for this large-scale comparative study have already been
108 published (Herfort et al., 2006; Huguet et al., 2007, 2011; Bendle et al., 2010; Fietz et
109 al., 2011a, 2011b). We discuss the possible mechanisms responsible for such a global

110 pattern, including the prospect that branched GDGTs have a significant autochthonous
111 source in some aquatic settings.

112

113

2. REGIONAL SETTINGS

114 The map in Figure 1 identifies the sites included in this paper and further information
115 on each sampling location is provided in Table 1. We show sediment trap, surface
116 sediment and downcore data from lakes in Russia, France, and Turkey, as well as data
117 for water column (filtered particulate matter), sediment trap, and surface and downcore
118 sediment samples from locations in the Atlantic, Pacific, North Sea, and Mediterranean.
119 Brief descriptions of all locations and data sets are given in Appendix 1.

120

121

3. MATERIAL AND METHODS

122 Sample processing methods are diverse as the data were obtained by different research
123 groups with a focus initially outside the scope of the present analysis. All methods are
124 briefly described, including those concerning already published data sets (Herfort et al.,
125 2006; Huguet et al., 2007, 2011; Escala 2009; Bendle et al., 2010; Fietz et al., 2011a,
126 2011b; McClymont et al., in press) so that they can be compared. The numbering given
127 for extraction, fractionation and analyses refer to the respective data sets listed in Table
128 1.

129

3.1. Lipid extraction

130 All samples were freeze-dried and sediments homogenized. Solvents used for extraction
131 were mixtures of dichloromethane and methanol (DCM/MeOH). **E1**) Microwave
132 assisted extraction (as in Huguet et al., 2007, 2011; Escala et al. 2009; Fietz et al.

133 2011a, 2011b; McClymont et al., in press), **E2**) Accelerated Solvent Extractor (ASE
134 200, Dionex; as in Herfort et al., 2006), **E3**) Ultrasonic extraction (as in Schouten et al.,
135 2007), **E4**) 24h Soxhlet extraction (as in Bendle et al., 2010).

136 **3.2. Fractionation, purification**

137 **F1**) Extracts were analyzed without further fractionation (as in Fietz et al., 2011a). **F2**)
138 Extracts were fractionated with preparative column chromatography using activated
139 alumina and sequential eluent mixtures of hexane (HEX)/DCM, HEX/DCM and
140 DCM/MeOH (as in Huguet et al., 2011). **F3**) Extracts were fractionated with
141 preparative column chromatography using activated or deactivated silica (1 or 5% H₂O)
142 and sequential eluents HEX, DCM or a mixture of HEX/DCM and DCM/MeOH (as in
143 Herfort et al., 2006). **F4**) Extracts were redissolved in HEX/DCM and injected in a
144 Thermo Surveyor HPLC system equipped with a Lichrosphere silica column.
145 Fractionation was achieved running sequentially HEX, DCM, and acetone (as in Fietz et
146 al. 2011a). **F5**) Extracts were hydrolyzed overnight with 8% potassium hydroxide
147 (KOH) in MeOH. The GDGT-containing fraction was recovered with hexane (as in
148 Escala, 2009). **F6**) Extracts were redissolved in chloroform and eluted through 500 mg
149 aminopropyl mini-columns running sequentially chloroform/2-propanol and diethyl
150 ether/acetic acid (as in Ruiz et al., 2004).

151 **3.3. Analysis**

152 All polar fractions were redissolved in HEX/n-propanol or HEX/isopropanol prior to
153 injection into the respective HPLC-MS system. All instruments used in this study were
154 equipped with an atmospheric pressure chemical ionization (APCI) source. Mixtures of
155 HEX/n-propanol or HEX/isopropanol were used as eluents either in gradient or isocratic
156 modes. **A1**) A Dionex P680 HPLC system coupled to a Thermo Finnigan TSQ

157 Quantum Discovery Max quadrupole mass spectrometer (MS) was used with a Tracer
158 Excel CN column (as in Fietz et al., 2011a, 2011b. **A2**) An Agilent 1100 HPLC system
159 coupled to a Bruker Esquire 3000 ion trap MS was used and a Nucleosil CN column (as
160 in Escala, 2009). **A3**) An HP 1100 Series HPLC-MS system was used and a Prevail
161 Cyano column (Herfort et al., 2006; Huguet et al., 2007). A3 analyses were done in
162 triplicate and averages are presented in this study. **A4**) An Agilent 1100 series/HP 1100
163 MSD series HPLC-MS system was used and an Alltech Prevail Cyano column (Bendle
164 et al., 2010). **A5**) A Thermo Finnigan LCQ MS was used with a Grace Prevail Cyano
165 column (McClymont et al., in press). GDGTs in all **A1-A5** analyses were monitored in
166 selected ion monitoring (SIM) mode at m/z 1302, 1300, 1298, 1296, 1292 (isoprenoidal
167 GDGTs, with 1292 referred here as crenarchaeol), 1050, 1036, and 1022 (major
168 branched GDGTs), and m/z 1048, 1046, 1034, 1032, 1020, and 1018 (minor, cyclized
169 branched GDGTs).

170 **3.4. Normalization**

171 Since we can not rule out artefacts in concentrations derived from the different
172 instrument and quantification methods used across the various laboratories included in
173 this study, all data were normalized and data are given here as relative units.
174 Normalization was accomplished by finding the sample with the highest crenarchaeol
175 relative unit in a given data set and then dividing all crenarchaeol and branched GDGT
176 data in that set to this reference value.

177 **3.5. TOC and chlorophyll**

178 For some sample sets, reference data for total organic carbon (TOC) and chlorophyll *a*
179 transformation products (including all pheopigments) were available, partly from
180 published studies (Herfort et al., 2006; Fietz et al., 2007, 2011a; Huguet et al., 2007,

181 2011; Martínez-Garcia et al., 2009). This information allows the data to be expressed
182 per gram TOC or per gram chlorophyll degradation products. For the Lake Baikal
183 interglacial record, TOC and chlorophyll transformation products analyses were carried
184 out on parallel samples (same core) to the above described GDGT analyses within an
185 earlier study (Fietz et al., 2007). TOC analyses for the Drammensfjord were carried out
186 on parallel samples to the above described GDGT analyses as described by Huguet et al.
187 (2007). Chlorophyll transformation products for sediment trap samples from Lake Van
188 (Huguet et al., 2011) and Lake Baikal, as well as downcore samples from Fram Strait
189 (Fietz et al., 2011a), subantarctic Atlantic (Martínez-Garcia et al., 2009), and Guaymas
190 Basin were measured on the total lipid extracts before further fractionation was carried
191 out for GDGT analyses. The method is described by Martínez-Garcia et al. (2009).

192

193

4. RESULTS

194 In almost all sample sets, the abundance of crenarchaeol is significantly ($p < 0.001$)
195 correlated to the combined abundance of the major branched GDGTs (Figures 2 and 3,
196 Table 1), as well as to the combined abundance of the minor cyclized branched GDGTs,
197 (Table 1). This strong correlation is observed in samples from freshwater and marine
198 environments at varying distances from the shore, over a range of redox conditions and
199 with different pathways of terrestrial matter input. No significant correlation between
200 crenarchaeol and branched GDGTs was found in only three out of the 30 data sets
201 examined in this study.

202

4.1. Data sets with significant correlations between crenarchaeol and branched

203

GDGTs

204

4.1.1. Lakes

205 Significant correlations ($p < 0.01$) are found in down core sediment sample sets from
206 Lake Baikal, Lake Bourget, and Lake Van even though different interglacial and glacial
207 cycles are considered, as well as in surface sediments and sediment trap material (Fig.
208 2). All correlations have coefficients of determination (r^2) higher than 0.8 and a wide
209 range of slope values (Table 1). Variation in slope values is indicative of the relative
210 concentration change between branched GDGTs and crenarchaeol. It must be noted that
211 in an intercalibration study (Schouten et al., 2009) the BIT index, which resembles the
212 slope of branched GDGTs versus crenarchaeol, varied greatly between individual LC-
213 MS systems (e.g., BIT values ranging from 0.25 to 0.82 on a scale from 0 to 1).
214 However, in the present study a wide range of slope values is also found for sample sets
215 measured on the same LC-MS (e.g., 0.4 to 4.1 for LC-MS system A1, see Table 1) and
216 the coefficient of variation (CV, calculated as standard deviation per mean value) is
217 higher for the lake slope values (CV=0.5) than for the BIT in the intercalibration study
218 (CV=0.2). Significant correlations are furthermore observed between cyclized branched
219 GDGTs and crenarchaeol in the lakes and the r^2 -values are only slightly lower than
220 those calculated for the major branched GDGT versus crenarchaeol correlations (Table
221 1).

222 *4.1.2. Marine Settings*

223 Significant correlations ($p < 0.01$) between the major brGDGTs and crenarchaeol are
224 observed in most downcore records of our marine sites (Fig. 3A-J), although the
225 environmental conditions as well as pathways and amounts of terrestrial matter input
226 strongly differ between the studied sites. All r^2 values are higher than 0.57 (Table 1).
227 Such strong correlation is not only found through time at certain sites, but also in two
228 surface sediment compilations of the North and Catalan Seas (Table 1, Figs. 3K,L). As
229 for lakes, slopes vary over a wide range (0.01 to 0.9; Table 1). Some sites that receive

230 more allochthonous material through eolian input (Guaymas Basin, equatorial Pacific,
231 subantarctic Atlantic) than by river discharge have shallow slopes (≤ 0.07). The
232 equatorial Atlantic site, however, which predominantly receives dust input from the
233 Sahara, has a remarkably steep slope of 0.61 (even though measured on the same LC-
234 MS than the subantarctic Atlantic samples that have a slope of 0.06, see Table 1).
235 Significant correlations are also observed between cyclized branched GDGTs and
236 crenarchaeol in the marine sites and again (as for lakes) the r^2 values are in a similar
237 range as those calculated for the major branched GDGT versus crenarchaeol
238 correlations (Table 1).

239 **4.2. Sites without significant correlation between crenarchaeol and major** 240 **branched GDGTs**

241 No significant correlation is found in two downcore records and one water column
242 sample set (Fig. 4). Lake Yamozero is, at present, a shallow lake with large lake level
243 variations, which have caused major hiatuses in the record (Henriksen et al., 2008). This
244 may explain the large scatter in the branched GDGTs vs. crenarchaeol correlation. The
245 NE Atlantic site lies within the impact zone of the British Ice Sheet and the record is
246 characterized by the sudden input of abundant and very ancient terrestrial organic matter
247 (Peck et al., 2006), which might have caused the scatter. Lack of significant correlation
248 is also observed in the water samples from Chipana, off Chile. One sample deviated
249 from the five others and this outlier (February 2007 surface sample) was mainly due to
250 low crenarchaeol concentration instead of exceptionally high branched GDGT
251 concentrations (Fig. 4).

252 **4.3. Correlation for data sets normalized to total organic carbon or chlorophyll** 253 **transformation products**

254 When possible, the GDGT data were normalized to TOC in order to assess the
255 possible impact of organic matter diagenesis on the correlation (Fig. 5). Where TOC
256 data are available, the brGDGTs/TOC vs. crenarchaeol/TOC correlations are still
257 significant at $p < 0.01$ (Baikal Interglacial, Buguldeyka Uplift, Drammensfjord and North
258 Sea; Fig. 5; Table 2). Yamamoto et al. (2008) and Zhu et al. (2011) both also published
259 significant correlations between TOC normalized branched GDGTs and crenarchaeol.
260 Only in one data set (Lake Van) the relationship between brGDGTs/TOC and
261 crenarchaeol/TOC is deteriorated ($p = 0.05$; Fig. 5, Table 2).

262 For many records, TOC data are not available. Chlorophyll *a* transformation products
263 (including phaeopigments) are considered instead, because they track the aquatic
264 primary productivity component of the deposited organic matter (Harris et al., 1996).
265 Chlorophyll *a* produced in the water column is strongly degraded before final burial and
266 hence, normalization to chlorophyll transformation products (Chl.) reduces the impact
267 of diagenesis in the data sets similarly to TOC. The fit of brGDGTs/Chl. versus
268 crenarchaeol/Chl. is still significant ($p < 0.01$) for Lake Baikal and Lake Van seasonal
269 traps, as well as for Lake Baikal Interglacial, Guaymas Basin, Fram Strait, and
270 subantarctic Atlantic records ($r^2 = 0.58-0.99$; Table 2).

271

272

5. DISCUSSION

273 Crenarchaeol is considered a marker for mesophilic Thaumarchaeota of predominantly
274 aquatic origin (Sinninghe Damsté et al., 2002), while branched GDGTs are proposed
275 markers for soil Bacteria (Weijers et al., 2010). Positive correlation between branched
276 GDGTs and crenarchaeol was reported previously for the Central Arctic (Yamamoto et
277 al., 2008) and the East China Sea shelf (Zhu et al., 2011). Since we observe it in all, but

278 three, of the 30 data sets examined here, this phenomenon is a global feature. The key
279 question to answer is: how can two markers from purportedly two different source
280 environments display such strong correlation in so many different settings?

281 **5.1. Amplification of correlation by diagenesis**

282 Preservational efficiency is an important factor to explain variability in downcore
283 sedimentary signals (Furlong and Carpenter, 1988; Calvert and Pedersen, 1992). Earlier
284 studies demonstrated that oxygen exposure can cause a decrease in GDGT
285 concentration by one or two orders of magnitude (Schouten et al., 2004; Zonneveld et
286 al., 2010). Amplification in the dry weight related concentrations due to the settling and
287 preservation conditions can therefore not be excluded as an explanation for the observed
288 correlations in the sedimentary data sets. However, if diagenetic factors primarily
289 control the biomarker concentrations, the significant correlation between brGDGTs and
290 crenarchaeol normalized to dry weight should be largely deteriorated when both are
291 normalized to TOC. GDGTs are associated to their respective organic matter sources.
292 Input, settling and preservation of GDGTs are therefore closely related to the TOC,
293 which contains aquatic and terrestrial compounds. TOC-normalization of the GDGTs
294 therefore minimizes temporal or regional variability in the amount of organic matter
295 deposited and/or changes in preservation conditions for given data sets. However, in
296 two Lake Baikal records, the Drammensfjord record and the North Sea surface sediment
297 compilation, the correlations between brGDGTs/TOC and crenarchaeol/TOC are
298 diminished but remain significant (Fig. 5, Table 2). brGDGTs/TOC and
299 crenarchaeol/TOC are also correlated in sample sets from the Central Arctic
300 (Yamamoto et al., 2008) and China Sea (Zhu et al., 2011). The regression is deteriorated
301 at insignificant level in only one data set (Lake Van). If plotted against chlorophyll
302 degradations products (chl.), which are also affected by the preservational conditions,

303 the correlations of brGDGTs/chl. versus crenarchaeol/chl. are also still significant
304 (Table 2).

305 Furthermore, diagenesis differs between branched and isoprenoid GDGTs. Huguet et
306 al. (2008) found that over long time spans (>100 ky) branched GDGTs are better
307 preserved than isoprenoidal GDGTs. At sites or time spans with lower overall
308 productivity and sedimentation, and therefore prevailing oxic conditions, the
309 brGDGTs/crenarchaeol ratio might thus be biased towards higher values. Such redox
310 condition dependant shift in the brGDGTs/crenarchaeol ratio should have reduced the
311 correlation. Therefore, diagenetic processes are probably not the primary driving factors
312 for the observed correlations.

313 **5.2. Correlations triggered by physical processes in different source** 314 **environments**

315 Very few environmental factors might have a direct and equal influence to both
316 aquatic Thaumarchaeota and GDGT-producing soil Bacteria. Temperature, for example,
317 which would be a global feature for soil and aquatic systems, has only been shown to be
318 of major influence for the relative distribution of isoprenoid GDGT distributions but not
319 for absolute abundances (Schouten et al., 2002). pH and anaerobic conditions have been
320 proposed as major environmental factors driving the concentration of branched GDGTs
321 in soils (Weijers et al., 2007), but there is no published study about what environmental
322 factor drives the crenarchaeol concentration in the aquatic settings.

323 The observed co-variations between crenarchaeol and branched GDGTs might instead
324 result to some extent from parallel or sequential effects. For example, if branched
325 GDGTs indicate allochthonous matter input, they would be coupled to nutrient input
326 which may result in site fertilization. A likely scenario to explain the co-variation

327 between branched GDGTs and crenarchaeol might therefore be that increases in
328 branched GDGTs would be an indicator of e.g., erosion, dust, or ice-rafted debris input.
329 This might serve as a substrate for the Thaumarchaeota or contain nutrients that fertilize
330 the system and induce increased deposition. However, it remains questionable if
331 fertilization can possibly explain the worldwide observed correlations, including sites
332 unlikely to be resource limited (e.g. Lake Baikal, Lake Bourget, Lake Van, North Sea).

333 **5.3. Correlations due to common source environment of both GDGT types**

334 A common terrestrial origin has been suggested by Yamamoto et al. (2008) for
335 crenarchaeol and branched GDGTs in central Arctic sediments. Yamamoto et al. (2008)
336 proposed that both types of GDGTs were introduced by terrestrial matter trapped in the
337 ice and released as the ice drifted and melted over the central Arctic. However, a
338 common terrestrial origin is an unlikely explanation for correlations observed globally.
339 In contrast, Zhu et al. (2011) suggested a common aquatic source for crenarchaeol and
340 branched GDGTs in the East China Sea. Co-variation of Thaumarchaeota and Bacteria
341 has been shown in water column studies based on metagenomic surveys (Beman et al.,
342 2011). Therefore, co-production of branched GDGTs in aquatic settings by Bacteria
343 may account for the observed correlation.

344 From the distribution of branched GDGTs in soils (Weijers et al. 2007, 2010), it
345 actually seems that they are produced by waterborne Bacteria as they seem to be found
346 predominantly around the water table or in soil pore water. Furthermore, brGDGT-
347 producing Bacteria have been proposed to be anaerobic (Weijers et al., 2006b). This
348 suggests that they could possibly also be produced in the water column (oxygen
349 minimum zone), at the sediment surface, or in anoxic interstitial spaces within the
350 sediments. Aquatic *in situ* production of branched GDGTs has been in fact suggested in

351 many earlier studies, predominantly in lakes (Sinninghe Damsté et al., 2009; Bechtel et
352 al., 2010; Blaga et al., 2010; Tierney et al., 2010; Zink et al., 2010; Sun et al., 2011),
353 and also in two marine settings (Peterse et al., 2009; Zhu et al., 2011).

354 **5.4. Mixed origins**

355 Part of the branched GDGTs detected in lakes and oceans must be of terrestrial origin
356 because in almost all aquatic settings there is evidently some terrestrial matter input
357 through erosion, river run-off, or wind transport. Furthermore, branched GDGTs and
358 crenarchaeol are not correlated if we pool all of the data into one global set, because of
359 the large differences in regression slopes. Partly these differences might be attributed to
360 the analytical constraints (Escala et al., 2009; Schouten et al., 2009). However, the
361 slopes varied over wide ranges even if analyzed with the same LC-MS (e.g., 0.06 and
362 0.6 for subantarctic Atlantic and equatorial Atlantic). Furthermore, the coefficient of
363 variation of our slope values is much higher (0.88) than for the BIT values in the
364 Schouten et al. (2009) intercalibration study (0.24), indicating that the slope values
365 range is beyond the LC-MS-based differences. Most slopes are higher in the lakes than
366 in the marine sites (Table 1). This could support the original premise that crenarchaeol
367 is autochthonous and branched GDGTs are allochthonous or indicate a higher *in situ*
368 production of branched GDGTs in lakes than in oceans or a combination of both. It is
369 therefore most likely that both GDGTs types have a mixed autochthonous and
370 allochthonous origin. This mixed origin has consequences for the use of GDGT derived
371 proxies for paleoclimatic reconstructions, as the reliability of both BIT and MBT/CBT
372 indices depends on the assumption that the branched GDGTs deposited in the sediments
373 are exclusively of terrestrial origin.

374

6. CONCLUSION

375

376 Until recently, it has been widely accepted that in sedimentary archives crenarchaeol is
377 predominantly derived from aquatic Archaea and branched GDGTs are derived from
378 soil Bacteria. In this study, we show that branched GDGTs are correlated to
379 crenarchaeol on a region by region basis in globally distributed records. Certainly, the
380 correlation is partly due to an amplification effect caused by preservation of both GDGT
381 types in sedimentary settings with high preservation potential, but diagenesis can not be
382 the one and only process driving the observed tight correlations. Various scenarios of
383 common physical driving factors or cascading effects are plausible to explain the
384 correlations at specific sites. Those are, however, not satisfying to explain the global
385 pattern. Globally considered, our findings of strong correlations coupled to a wide range
386 of slopes indicate a more complex situation, suggesting that a mixed source for both
387 GDGT types is commonplace in lacustrine and marine settings.

388

389 *Acknowledgements:* N. Moraleda is thanked for sample processing and analysis. The
390 authors thank R. Gyllencreutz, R. Spielhagen, A. Prokopenko, J. Jacob for providing
391 samples. The authors furthermore thank teams from CONTINENT, IMAGES IV,
392 MONA, and ANTROMARE. J.B. thanks the staff and colleagues at the NERC Life
393 Sciences Mass Spectrometry Facility (Bristol), the Organic Geochemistry Unit at
394 University of Bristol, and the Department of Marine Organic Biogeochemistry at Royal
395 Netherlands Institute for Sea Research (NIOZ).

396 S.F. thanks the Deutsche Forschungsgemeinschaft (DFG) for a Postdoctoral
397 Fellowship (FI 1466/1-1). S.F. and C.H. thank the Spanish Ministerio de Ciencia e
398 Innovación (MICINN) for Juan de la Cierva fellowships. M.E. thanks the Generalitat de
399 Catalunya. J.B. thanks the Natural Environment Research Council (NE/C508934/1), the
400 Ocean Drilling Programme (IODP), The Carnegie Trust for the Universities of
401 Scotland, and the Projects ‘Millennium’ and IMAGES. E.L.M. thanks Natural
402 Environment Research Council (NE/E00119X/1) and the IMAGES programme. A.M.G.
403 and G.R. thank the MICINN (AP2004-7151 and AP2008-00801). F.P. acknowledges
404 support from the National Science Foundation sponsored Center for Coastal Margin
405 Observation and Prediction. S.R. was co-financed with Beatriu de Pinós (2006 BP-B1
406 00069) and Ramón y Cajal Contracts (RyC-2007-01327). A.R.M. acknowledges
407 support from the European Commission Marie Curie-IOF (235626). Support for this
408 work was furthermore provided by the MICINN as research funds (POL2006-02990,
409 CGL2008-03288-E, CGL2010-15000).

410 **REFERENCES**

- 411 Bechtel, A., Smittenberg, R.H., Bernasconi, S.M., Schubert, C.J., 2010. Distribution of
412 branched and isoprenoid tetraether lipids in an oligotrophic and a eutrophic Swiss
413 lake: Insights into sources and GDGT-based proxies. *Org. Geochem.* 41, 822-832.
- 414 Beman, J.M., Steele, J.A., and Fuhrman J.A., 2011. Co-occurrence patterns for
415 abundant marine archaeal and bacterial lineages in the deep chlorophyll maximum of
416 coastal California. *ISME J.* 5, 1077–1085.
- 417 Bendle, J.A., Weijers, J.W.H., Maslin, M.A., Sinninghe, Damsté J.S., Schouten, S.,
418 Hopmans, E.C., Boot, C.S. and Pancost, R.D., 2010. Major changes in glacial and
419 Holocene terrestrial temperatures and sources of organic carbon recorded in the
420 Amazon fan by tetraether lipids. *Geochem. Geophys. Geosyst.* 11, Q12007,
421 doi:10.1029/2010GC003308
- 422 Blaga, C.I., Reichart, G.-I., Schouten, S., Lotter, A.F. Werne, J.P., Kosten, S., Mazzeo ,
423 N., Lacerot, G., Sinninghe Damsté, S.J., 2010. Branched glycerol dialkyl glycerol
424 tetraethers in lake sediments: Can they be used as temperature and pH proxies? *Org.*
425 *Geochem.* 41, 1225-1234.
- 426 Brochier-Armanet, C., Boussau, B., Gribaldo, S., Forterre, P., 2008. Mesophilic
427 Crenarchaeota: proposal for a third archaeal phylum, the Thaumarchaeota,
428 *Nat. Rev. Microbiol.* 6, 245-52.
- 429 Calvert, S.E., Pedersen, T.F., 1992. Organic matter accumulation, remineralization and
430 burial in an anoxic coastal sediment. In: Whelan, J.K., Farrington, J.W. (Eds.),
431 *Organic Matter: Productivity, Accumulation and Preservation in Recent and Ancient*
432 *Sediments.* Columbia Univ. Press, New York, pp. 231–263.
- 433 Casamayor, E.O., Borrego C.M., 2009. Archaea in inland waters. In: Likens G. (Ed.),
434 *Encyclopedia of Inland Waters.* Academic Press, Elsevier UK, vol. 3, pp. 167-181.
- 435 DeLong, E.F., 1998. Everything in moderation: archaea as ‘non-extremophiles’. *Curr.*
436 *Opin. Genet. Dev.* 8, 649–654.
- 437 Escala, M., 2009. Application of tetraether membrane lipids as proxies for continental
438 climate reconstruction in Iberian and Siberian lakes. Ph. D. thesis, Universitat
439 Autònoma de Barcelona (<http://www.tdx.cat/TDX-1020109-144857>)
- 440 Escala, M., Fietz, S., Rueda, G., Rossell-Melé, A., 2009. Analytical considerations for
441 the use of the paleothermometer Tetraether Index₈₆ and the Branched vs Isoprenoid
442 Tetraether Index regarding the choice of cleanup and instrumental conditions. *Anal.*
443 *Chem.* 81, 2701–2707.
- 444 Fietz, S., Nicklisch, A., Oberhänsli, H., 2007. Phytoplankton response to climate
445 changes in Lake Baikal during the Holocene and Kazantsevo Interglacials assessed
446 from sedimentary pigments. *J. Paleolimn.* 37, 177-203.
- 447 Fietz, S., Martínez-García, A., Rueda, G., Peck, V.L., Huguet, C., Escala, M., Rosell-
448 Melé, A., 2011a. Crenarchaea and phytoplankton coupling: Common trigger or
449 metabolic dependence? *Limnol. Oceanogr.* 56, 1907-1916.
- 450 Fietz, S., Martínez-García, A., Huguet, C., Rueda, G., Rosell-Melé, A., 2011b,
451 Constraints in the application of the Branched and Isoprenoid Tetraether (BIT) index
452 as a terrestrial input proxy, *J. Geophys. Res.* 116, C10032
453 doi:10.1029/2011JC007062.
- 454 Fuhrman, J.A., McCallum, K., Davis, A.A., 1992. Novel major archaeobacterial group
455 from marine plankton. *Nature* 356, 148–149.
- 456 Furlong, E.T., Carpenter, R., 1988. Pigment preservation and remineralization in oxic
457 coastal marine sediments. *Geochim. Cosmochim. Ac.* 52, 87–99.
- 458 Gattinger, A., Günthner, A., Schloter, M., Munch, J.C., 2003. Characterisation of
459 Archaea in soils by polar lipid analysis. *Acta Biotechnol.* 23, 21-28.

460 Harris, P.G., Zhao, M., Rosell-Melé, A., Tiedemann, R., Sarnthein, M., Maxwell, J.R.
461 1996. Chlorin accumulation rate as a proxy for Quaternary marine primary
462 productivity. *Nature* 383, 63–65.

463 Henriksen, M., Mangerud, J., Matiouchkov, A., Murray, A.S., Paus, A., Svendsen, J.I.
464 2008. Intriguing climatic shifts in a 90 kyr old lake record from northern Russia.
465 *Boreas* 37, 20–37.

466 Herfort, L., Schouten, S., Boon, J.P., Woltering, M., Baas, M., Weijers, J.M.H., and
467 Sinninghe Damsté, J.S., 2006. Characterization of transport and deposition of
468 terrestrial organic matter in the southern North Sea using the BIT index. *Limnol.*
469 *Oceanogr.* 51, 2196–2205.

470 Hopmans, E.C., Weijers, J.W.H., Schefuss, E., Herfort, L., Sinninghe Damsté, J.S.,
471 Schouten S., 2004. A novel proxy for terrestrial organic matter in sediments based on
472 branched and isoprenoid tetraether lipids. *Earth Planet. Sc. Lett.* 224, 107–116.

473 Huguet, C., Smittenberg, R.H., Boer, W., Sinninghe Damsté, J.S., and Schouten, S.
474 2007. Twentieth century proxy records of temperature and soil organic matter input
475 in the Drammensfjord, southern Norway. *Org. Geochem.* 38, 1838-1849.

476 Huguet, C., de Lange, G.J., Middelburg, J.J., Sinninghe Damsté, J.S., Schouten, S.
477 2008. Selective preservation of soil organic matter in oxidized marine sediments
478 (Madeira Abyssal Plain). *Geochim. Cosmochim. Acta* 72, 6061-6068.

479 Huguet, C., Fietz, S., Stockhecke, M., Sturm, M., Anselmetti, F.S., Rosell-Mele, A.
480 2011. Biomarker seasonality study in Lake Van, Turkey. *Org. Geochem.* 42, 1289-
481 1298.

482 Keough, B.P., Schmidt, T.M., Hicks, R.E., 2003. Archaeal nucleic acids in picoplankton
483 from great lakes on three continents. *Microb. Ecol.* 46, 238–248.

484 Kim, J.-H., Meer, J.v.d., Schouten, S., Helmke, P., Willmott, V., Sangiorgi, F., Koç, N.,
485 Hopmans, E.C., and Sinninghe Damsté, J.S., 2010. New indices and calibrations
486 derived from the distribution of crenarchaeol isoprenoid tetraether lipids:
487 implications for past sea surface temperature reconstructions. *Geochim. Cosmochim.*
488 *Ac.* 74, 4639–4654.

489 Leininger, S., Urich, T., Schloter, M., Schwark, L., Qi, J., Nicol, G.W., Prosser, J.I.
490 Schuster, S. C., Schleper, C., 2006. Archaea predominate among ammonia-oxidizing
491 prokaryotes in soils. *Nature* 442, 806-809.

492 Martínez-García, A., Rosell-Melé, A., Geibert, W., Gersonde, R., Masqué, P., Gaspari,
493 V., Barbante, C., 2009. Links between iron supply, marine productivity, sea surface
494 temperatures and CO₂ over the last 1.1My. *Paleoceanography*, PA1207. DOI:
495 10.1029/2008PA001657

496 Massana, R., DeLong, E.F., Pedros-Alio, C., 2000. A few cosmopolitan phylotypes
497 dominate planktonic archaeal assemblages in widely different oceanic provinces.
498 *Appl. Environ. Microbiol.* 66, 1777–1787.

499 McClymont E.L., Ganeshram R., Pichevin L.E., Talbot H.M., van Dongen B.E.,
500 Thunell R.C., Haywood A.M., Singarayer J.S., Valdes P.J., *in press*. Sea-surface
501 temperature records of Termination 1 in the Gulf of California: challenges for
502 seasonal and inter-annual analogues of tropical Pacific climate change
503 (2011PA002226).

504 Peck, V. L., Hall, I., Zahn, R., Elderfield, H., Grousset, F., Hemming, S.R., Scourse,
505 J.D., 2006. High resolution evidence for linkages between NW European ice sheet
506 instability and Atlantic Meridional Overturning Circulation. *Earth Planet. Sc. Lett.*
507 243, 476-488.

508 Peterse, F., Kim, J.-H., Schouten, S., Klitgaard Kristensen, D., Koç, N., Sinninghe
509 Damsté, J.S., 2009. Constraints on the application of the MBT/CBT

510 paleothermometer at high latitude environments (Svalbard, Norway). *Org. Geochem.*
511 40, 692-699.

512 Powers, L.A., Werne, J.P., van der Woude, A.J., Sinninghe Damsté, J.S., Hopmans,
513 E.C., and Schouten, S., 2010. Applicability and calibration of the TEX₈₆
514 paleothermometer in lakes. *Org. Geochem.* 41, 404–413.

515 Ruiz, J., Antequera, T., Andres, A.I., Petron, M.J., Muriel, E., 2004. Improvement of a
516 solid phase extraction method for analysis of lipid fractions in muscle foods. *Anal.*
517 *Chim. Acta* 520, 201-205.

518 Schleper, C., Holben, W., Klenk, H.-P., 1997. Recovery of crenarchaeotal ribosomal
519 DNA sequences from freshwater-lake sediments. *Appl. Environ. Microbiol.* 63, 321-
520 323.

521 Schlitzer, R., 2001. Ocean Data View, <http://www.awi-bremerhaven.de/GEO/ODV>

522 Schouten, S., Hopmans, E.C., Schefuß, E., Sinninghe Damsté, J.S., 2002. Distributional
523 variations in marine crenarchaeotal membrane lipids: a new tool for reconstructing
524 ancient sea water temperatures? *Earth Planet. Sc. Lett.* 204, 265–274.

525 Schouten, S., Hopmans, E.C., Sinninghe Damsté, J.S., 2004. The effect of maturity and
526 depositional redox conditions on archaeal tetraether lipid palaeothermometry. *Org.*
527 *Geochem.* 35, 567-571.

528 Schouten, S., Hugué, C., Hopmans E.C., Kienhuis M.V.M., Sinninghe Damsté J.S.,
529 2007. Analytical methodology for TEX₈₆ paleothermometry by high-performance
530 liquid chromatography/atmospheric pressure chemical ionization-mass spectrometry.
531 *Anal. Chem.* 79, 2940-2944.

532 Schouten, S., Hopmans, E.C., van der Meer, J., Mets, A., Bard, E., Bianchi, T.S.,
533 Diefendorf, A., Escala, M., Freeman, K.H., Furukawa, Y., Hugué, C., Ingalls, A.,
534 Ménot-Combes, G., Nederbragt, A.J., Oba, M., Pearson, A., Pearson, E.J., Rosell-
535 Melé, A., Schaeffer, P., Shah, S.R., Shanahan, T.M., Smith, R.W., Smittenberg, R.,
536 Talbot, H.M., Uchida, M., Van Mooy, B.A.S., Yamamoto, M., Zhang, Z.H.,
537 Sinninghe Damsté, J.S., 2009. An interlaboratory study of TEX₈₆ and BIT analysis
538 using high-performance liquid chromatography-mass spectrometry. *G-Cubed* 10,
539 Q03012, doi:10.1029/2008GC002221.

540 Sinninghe Damsté, J.S., Hopmans, E.C., Schouten, S., van Duin, A.C.T., Genevasen,
541 J.A.J., 2002. Crenarchaeol: The characteristic glycerol dibiphytanyl glycerol
542 tetraether membrane lipid of cosmopolitan pelagic Crenarchaeota. *J. Lipid Res.* 43,
543 1641–1651.

544 Sinninghe Damsté, J.S., Ossebaar, J., Abbas, B., Schouten, S., Verschuren, D., 2009.
545 Fluxes and distribution of tetraether lipids in an equatorial African lake: Constraints
546 on the application of the TEX₈₆ palaeothermometer and BIT index in lacustrine
547 settings. *Geochim. Cosmochim. Ac.* 73, 4232-4249.

548 Sinninghe Damsté, J.S., Rijpstra, W.I.C., Hopmans, E.C., Weijers, J.W.H., Foesel,
549 B.U., Overmann, J., Dedysh, S.N., 2011. 13,16-Dimethyl octacosanedioic acid (iso-
550 diabolic acid), a common membrane-spanning lipid of Acidobacteria subdivisions 1
551 and 3. *Appl. Environ. Microbiol.* 77, 4147-4154.

552 Sun, Q., Chu, G., Liu, M., Xie, M., Li, S., Ling, Y., Wang, X., Shi, L., Jia, G., Lü, H.,
553 2011. Distributions and temperature dependence of branched glycerol dialkyl
554 glycerol tetraethers in recent lacustrine sediments from China and Nepal. *J. Geophys.*
555 *Res.* 116, G01008, doi:10.1029/2010JG001365.

556 Tierney, J.E., Russell, J.M., Eggermont, H., Hopmans, E.C., Verschuren, D., Sinninghe
557 Damsté, J.S., 2010. Environmental controls on branched tetraether lipid distributions
558 in tropical East African lake sediments. *Geochim. Cosmochim. Ac.* 74, 4902-4918.

- 559 Weijers, J.W.H., Schouten, S., Spaargaren, O., Sinninghe Damsté, J.S., 2006a.
560 Occurrence and distribution of tetraether membrane lipids in soils: Implications for
561 the use of the TEX₈₆ proxy and the BIT index. *Org. Geochem.* 37, 1680-1693.
- 562 Weijers, J.W.H., Schouten, S., Hopmans, E.C., Geenevasen, J.A.J., David, O.R.P.,
563 Coleman, J.M., Pancost, R.D., Sinninghe Damsté, J.S., 2006b. Membrane lipids of
564 mesophilic anaerobic bacteria thriving in peats have typical archaeal traits. *Environ.*
565 *Microbiol.* 8, 648–657.
- 566 Weijers, J.W.H., Schouten, S., van den Donker, J.C., Hopmans, E.C., Sinninghe
567 Damsté, J.S., 2007. Environmental controls on bacterial tetraether membrane lipid
568 distribution in soils. *Geochim. Cosmochim. Ac.* 71, 703-713.
- 569 Weijers, J.W.H., Wiesenberg, G.L.B., Bol, R., Hopmans, E.C., Pancost, R.D., 2010.
570 Carbon isotopic composition of branched tetraether membrane lipids in soils suggest
571 a rapid turnover and a heterotrophic life style of their source organism(s).
572 *Biogeosciences* 7, 2959-2973.
- 573 Yamamoto, M., Okino, T., Sugisaki, S., Sakamoto, T., 2008. Late Pleistocene changes
574 in terrestrial biomarkers in sediments from the central Arctic Ocean. *Org. Geochem.*
575 39, 754-763.
- 576 Zink, K.-G., Vandergoes, M. J., Mangelsdorf, K., Dieffenbacher-Krall, A. C., Schwark,
577 L., 2010. Application of bacterial glycerol dialkyl glycerol tetraethers (GDGTs) to
578 develop modern and past temperature estimates from New Zealand lakes. *Org.*
579 *Geochem.* 41, 1060-1066.
- 580 Zhu, C., Weijers, J.W.H., Wagner, T., Pan, J.-M., Chen, J.-F., Pancost, R.D., 2011.
581 Sources and distributions of tetraetherlipids in surface sediments across a large river-
582 dominated continental margin. *Org. Geochem.* 42, 376-386.
- 583

584

TABLES

585

586 **Table 1. Sites, Methods and Regression details:** Locations (numbers refer to map in
587 Figure 1) and methodologies (referring to numbers in the ‘Material and Methods’
588 section) as well as references for previously published data sets. Regression details are
589 given for plots shown in Figures 2 and 3 for the correlation of brGDGTs (sum of m/z
590 1050, 1036, and 1022) vs. crenarchaeol. Statistics are given here as well for cyclized
591 brGDGTs vs. crenarchaeol (sum of m/z 1020, 1028, 1034, 1032, 1048, and 1046; not
592 shown in Figures). Cyclised brGDGTs were, however, not analysed for all sample sets
593 and “not determined” (nd) refers to sites where they were not. Brief site and data set
594 descriptions are shown in Appendix 1. Abbreviations: Ref. – References; Ext. –
595 extraction methods; Fract. – fractionation methods; Anal. – analytical methods.; n -
596 number of samples included; nd – not determined; ns – not significant. Coefficients of
597 determination and slopes are only given if statistically significant ($p < 0.01$).

Data set	codes in Fig. 1	Methods		Latitude (°N)	Longitude (°E)	water depth (m)	Ref. for previously published GDT data	Regression statistics					
		Ext.	Fract.					Anal.	n	r ²	slope	r ²	slope
Lacustrine samples													
Lake Baikal:													
North - Holocene	L1	E1	F2	A1	54.0	108.9	386	Fietz et al. (2011b)	21	0.96	0.44	0.92	0.12
North - Last glacial	"	E1	F2	A1	"	"	"	"	60	0.80	0.46	0.83	0.18
North - Last interglacial	"	E1	F2	A1	"	"	"	Fietz et al. (2011a,b)	47	0.82	0.69	0.68	0.18
North - seasonal trap	L1	E1	F2	A1	54.5	109.1	920	"	6	0.94	0.42	ns	
North - annual trap	"	E1	F5	A2	"	"	"	"	6	0.97	0.13	0.92	<0.001
North - surface sediment	"	E1	F5	A2	"	"	"	"	10	0.98	0.15	ns	
South - Holocene	L2	E1	F5	A1	51.6	104.9	675	"	67	0.86	0.39	0.77	0.06
South - seasonal trap	L2	E1	F2	A1	51.7	105.0	1396	"	8	0.95	0.41	ns	
South - annual trap	"	E1	F5	A2	"	"	"	"	13	0.996	0.04	ns	
South - surface sediment	"	E1	F5	A2	"	"	"	"	10	0.99	0.51	0.97	<0.001
Centre - core	L3	E1	F5	A1	52.5	106.2	355	"	60	0.74	0.49	nd	
other lakes:													
Yamozero - core	L4	E1	F5	A2	65.0	50.1	3	"	22	0.95	0.41	0.94	0.15
Bourget - core	L5	E1	F5	A2	45.8	5.8	106	"	8	0.81	4.08	nd	
Van - seasonal trap	L6	E1	F2	A1	38.6	42.8	440	Hugnet et al. (2011)	8	0.81	4.08	nd	
Marine samples													
water column and surface sediment													
Chipana - POM	W1	E1	F6	A1	-21.3	-70.1	90	"	39	0.74	0.53	nd	
North Sea - surface sediment	S1	E2	F2	A3	53 to 55	3 to 4.3	24 to 47	Herfort et al. (2006)	24	0.95 ^a	0.10	nd	
Catalan Sea - surface sediment	S2	E1	F3	A1	39 to 41	-2 to -2.7	135 to 785	"	10	0.75	0.03	nd	
downcore sediment:													
Loch Sunart	C1	E3	F2, F3	A5	56.7	-5.9	50	"	41	0.89	0.03	nd	
Drummenfjord	C2	E2	F2	A3	59.7	10.4	100	Hugnet et al. (2007b)	76	0.95	0.11	0.94	0.07
Skagerrak 2007	C3	E1	F5	A2	58.7	10.2	225	"	28	0.85	0.20	0.90	0.16
Skagerrak 2008	"	E1	F2	A1	"	"	"	McClymont et al. (in press)	146	0.81	0.02	nd	
Guaymas Basin	C4	E1	F5	A5	27.5	-112.1	881	Bendle et al. (2010)	43	0.65	0.91	0.60	0.10
Amazon Fan	C5	E4	F2	A4	5.8	-49.1	3346	"	5	0.999	0.12	0.999	0.06
Alaskan coast	C6	E1	F2	A1	55.6	-133.5	200	"	43	0.57	0.07	0.57	0.07
Fram Strait	C7	E1	F4	A1	78.9	6.8	1490	Fietz et al. (2011a)	30	0.79	0.01	ns	
NE Atlantic	C8	E1	F2	A1	51.8	-12.9	1153	Fietz et al. (2011a)	127	0.89	0.06	0.82	0.05
equatorial Pacific	C9	E1	F1	A5	-1.6	-90.4	2580	"	50	0.74	0.02	0.89	0.01
subantarctic Atlantic	C10	E1	F1	A1	-42.9	9.0	3794	Fietz et al. (2011a,b)	10	0.84	0.61	0.94	0.20
Benguela current	C11	E1	F5	A1	13.0	-25.5	1992	"	10	0.84	0.61	0.94	0.20
equatorial Atlantic	C12	E1	F3	A1	3.0	-19.7	4849	"	10	0.84	0.61	0.94	0.20

^a significant if one station, influenced by the English coastal current and turbidity plume, is omitted (Fig. 3K)

600 **Table 2. Correlation statistics for major branched GDGTs versus crenarchaeol as**
601 **related to total organic carbon (TOC; cf. Fig. 5) or to chlorophyll transformation**
602 **products (CHL):** Number of samples included (n), coefficients of determination (r^2)
603 and slopes. All correlations and slopes are significant with $p < 0.001$, if not stated
604 otherwise. Details of the respective sample sets are given in Table 1. All data are
605 normalized. Normalization was accomplished by finding the sample with the highest
606 crenarchaeol/TOC concentration in a given sample set and then dividing all
607 crenarchaeol/TOC and brGDGTs/TOC data in that set by that value. The same
608 normalization was applied for the concentrations related to chlorophyll transformation
609 products. The GDGT, TOC and pigment concentration data were partly published
610 previously (Herfort et al., 2006; Huguet et al., 2007, 2011; Fietz et al., 2007, 2011;
611 Martínez-García et al., 2009).

612

		major brGDGTs/TOC vs. crenarchaeol/TOC		major brGDGTs/CHL. vs. crenarchaeol/CHL.	
	ref. Fig. 1	n	r^2	n	r^2
Lake Baikal North Interglacial	L1	44	0.50	46	0.97
Lake Baikal Centre	L3	44	0.81	-	-
Baikal seasonal trap (North)	L1	-	-	6	0.99
Baikal seasonal trap (South)	L2	-	-	8	0.95
Lake Van seasonal trap	L6	8	0.50 ^a	8	0.96
Drammensfjord	C2	41	0.81	-	-
Guaymas Basin	C4	-	-	144	0.84
Fram Strait	C7	-	-	43	0.77
subantarctic Atlantic	C10	-	-	126	0.40 ^b
North Sea surface sediment compilation	S1	21	0.88	-	-

^a $p=0.05$

^b $r^2=0.94$ if only glacial periods are considered (n=69)

613

614 **FIGURES**

615 **Figure 1.** Map showing all sample locations; codes refer to Table 1. Map created using
616 Ocean Data View (Schlitzer, 2001).

617 **Figure 2.** Correlations between crenarchaeol and branched GDGT concentrations per
618 gram dry weight in lakes with significant ($p < 0.01$) correlation. Lake Baikal (A) long-
619 term records from North Basin (Fietz et al., 2011a,b), (B) long-term record from
620 Buguldeyka uplift, (C) 10 cm upper surface sediment from South and North basins
621 (Escala 2009), and (D) annual and monthly sediment traps from South and North
622 basins; (E) Lake Bourget downcore record, and (F) Lake Van seasonal traps (Huguet et
623 al., 2011). See Figure 1 for locations, Table 1 for site details and Appendix 1 for brief
624 data set descriptions. Coefficients of determination (r^2) and slopes (x) are given for each
625 data set. See also Table 1 for more regression details. All data are normalized and given
626 here as relative units. Normalization was accomplished by finding the sample with the
627 highest crenarchaeol value in a given sample set and then dividing all crenarchaeol and
628 brGDGT data in that set by that value.

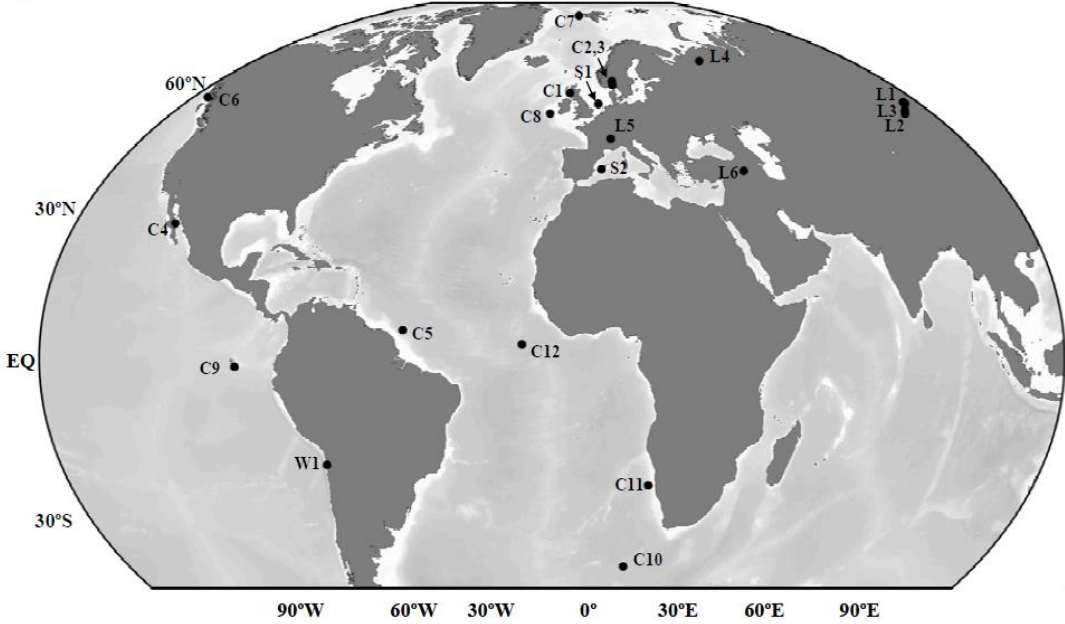
629 **Figure 3.** Correlations between crenarchaeol and branched GDGT concentrations per
630 gram dry weight in marine sites with significant ($p < 0.001$) correlation. (A-J) downcore
631 records, (K-L) surface sediment sets (0-1cm). In the North Sea surface sediment
632 compilation (K) the linear regression is given for samples influenced by the Dutch
633 Coast and Channel waters (DCC) omitting the station Central Southern Bight (CSB)
634 influenced by the English Channel and Turbidity plume (see Herfort et al., 2006). Some
635 data sets were previously published (Herfort et al., 2006; Huguet et al., 2007; Bendle et
636 al., 2010; Fietz et al, 2011a, 2011b). Coefficients of determination (r^2) and slopes (x) are
637 given for each data set. See Figure 2 legend for site, regression and normalization
638 details.

639 **Figure 4.** Sites without significant correlation between crenarchaeol and branched
640 GDGT concentrations per gram dry weight ($p>0.01$). See Figure 2 legend for site and
641 normalization details.

642 **Figure 5.** Correlations between crenarchaeol and branched GDGT normalized to total
643 organic carbon (TOC) in (A) Lake Baikal North Basin Interglacial record, (B) Lake
644 Baikal Buguldeyka uplift Holocene record, (C) Lake Van seasonal traps, (D)
645 Drammensfjord record, and (E) North Sea surface sediment (0-1cm) compilation. In the
646 North Sea surface sediment compilation (K) the linear regression is given for samples
647 influenced by the Dutch Coast and Channel waters (DCC) omitting the station Central
648 Southern Bight (CSB) influenced by the English Channel and Turbidity plume (see
649 Herfort et al., 2006). Data were partly published previously (Herfort et al., 2006;
650 Huguet et al., 2007, 2011; Fietz et al., 2011a, 2011b). See Figure 2 legend for site,
651 regression and normalization details.

652

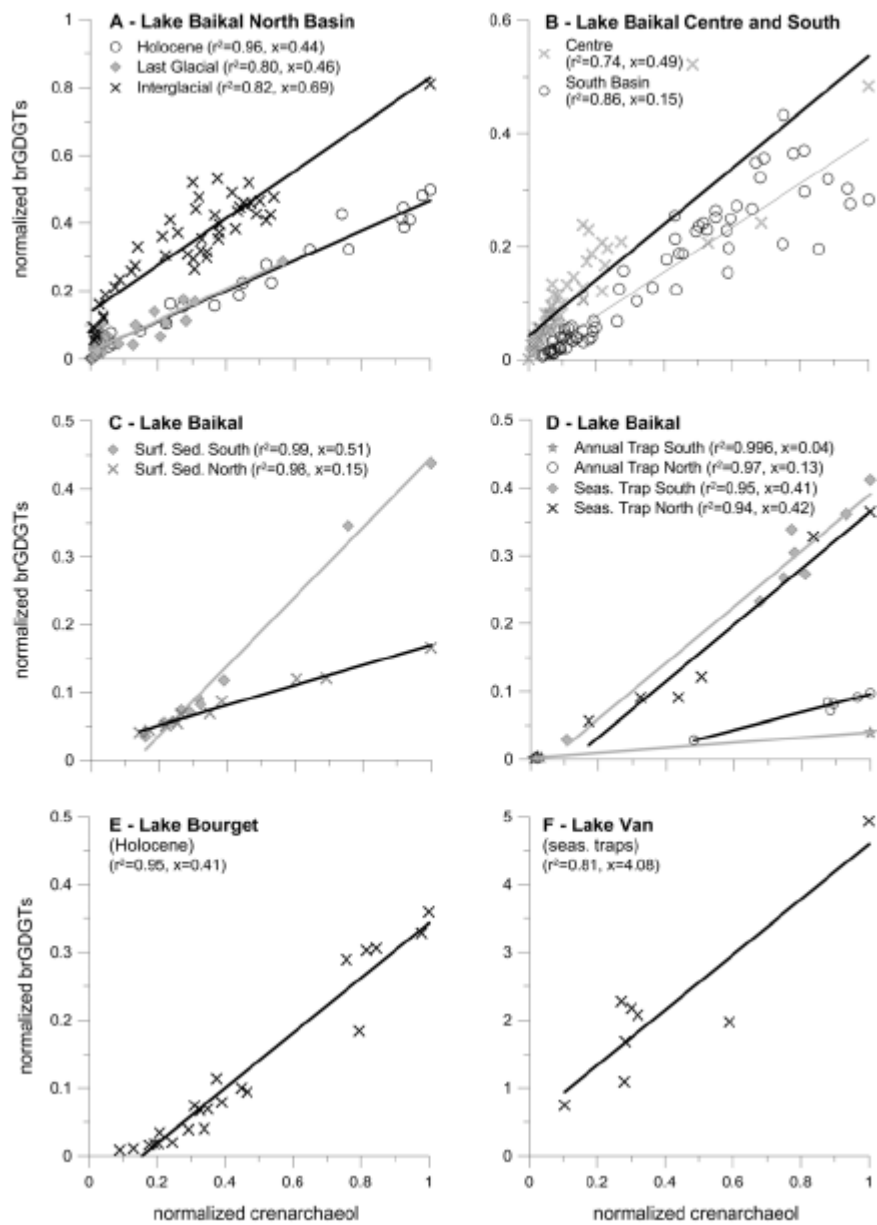
Figure 1



653

654

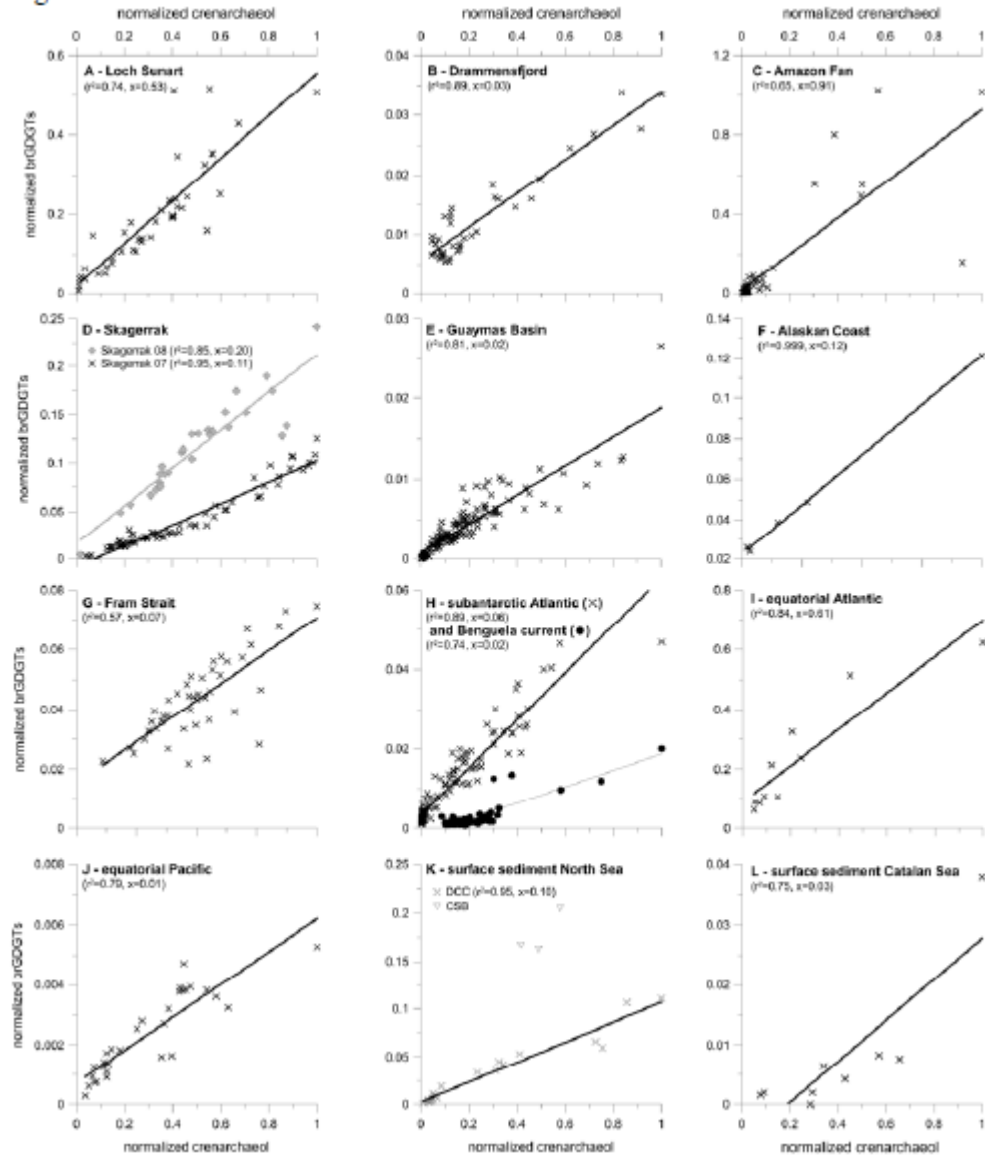
Figure 2



655

656

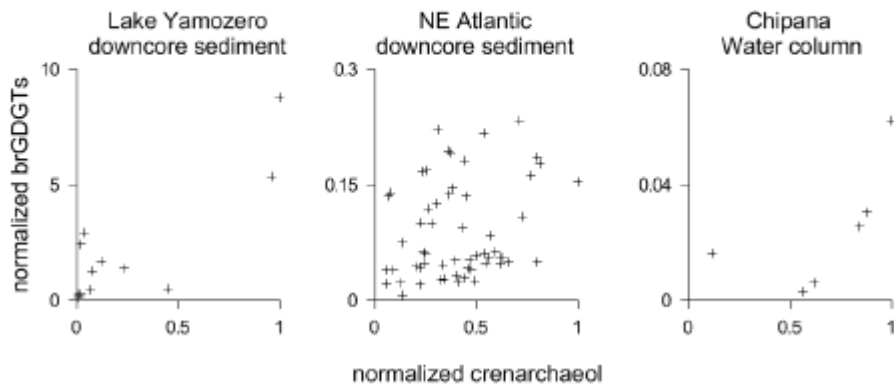
Figure 3



657

658

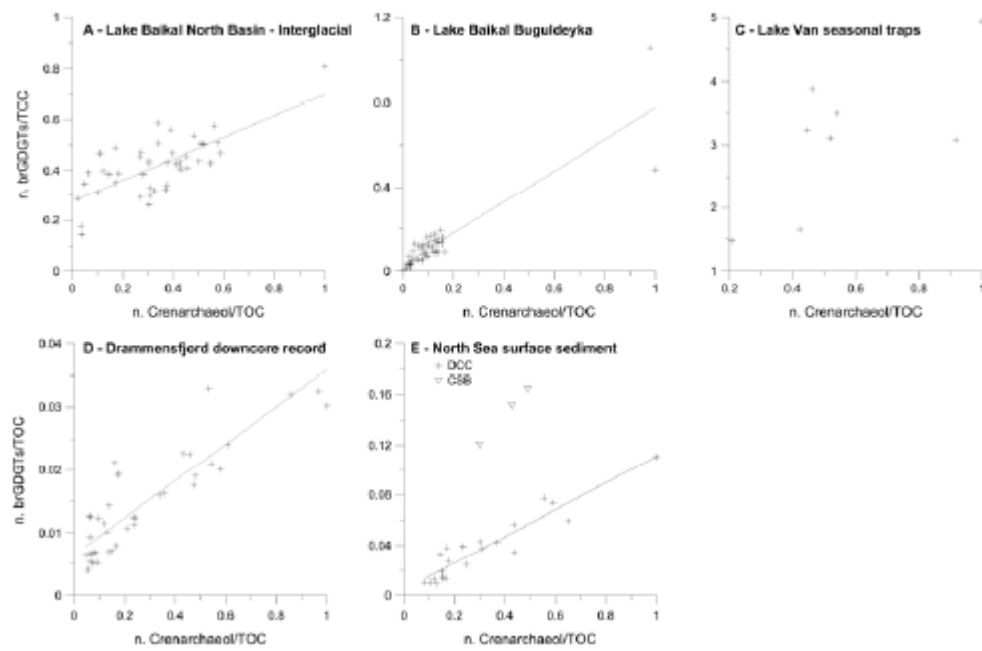
Figure 4



659

660

Figure 5



661

662

663 **Appendix 1:** Brief description of each sampling location and data set (e.g., geographic
664 location, major environmental features, time span of data set for sediment cores or
665 deployment of traps, and reference literature).

666 **1. Lacustrine samples**

667 *Lake Baikal* (central Siberia) is the World's deepest lake (ca. 1.6 km) and also one of
668 the largest (ca. 600 km long). The water column remains oxygenated throughout the
669 year. The lake is oligotrophic with periodic massive diatom blooms (Kozhov and
670 Izmet'yeva, 1998). The Selenga River is the largest tributary into the central lake and
671 has built up an enormous delta region. Lake Baikal downcore sediments were recovered
672 from the North and South Basins (Oberhänsli and Mackay, 2005), and from the
673 Buguldeyka Uplift in front of the Selenga Delta (Karabanov et al., 2008). The North
674 Basin Last Interglacial record spans ca. 113-129 thousand years before present (ky BP;
675 Fietz et al. 2007), the North Basin Last Glacial record spans ca. 12-57 ky BP, and the
676 North Basin Holocene record the last 12 ky. The South Basin and Buguldeyka Uplift
677 records also cover the Holocene but only part of the Last Glacial (<30 ky). Two surface
678 sediment cores (upper 10 cm) were recovered in 2001 from the North and South basins.
679 Both coring sites are located at a distance of ca. 400 km from each other. The North is
680 ice covered for longer and has a shorter vegetation period than the South, and it has an
681 overall lower sedimentation rate resulting in deeper oxic and oxygenized sediment
682 depth (Müller et al., 2005). Annually integrating sediment traps were deployed in June
683 2001 at 6 different depths along the 920 m deep water column in the North, and at 14
684 different depths along the 1396 m deep water column in the South (Fietz et al. 2005).
685 Seasonal traps were deployed on the same moorings than the annually integrating traps
686 below the upper mixed water layers and above the lake bottom.

687 *Lake Yamozero*, located in northern Siberia outside the present zone of permafrost,
688 covers an area of c. 30 km², and has an almost circular outline with a maximum water
689 depth of ca. 3 m (Henriksen et al., 2008). The small catchment area of 95 km² consists
690 of mires near the shore and a boreal forest (Henriksen et al., 2008). A series of distinct
691 shorelines encircles the lake up to a level of about 15 m above the present lake level
692 (Henriksen et al., 2008). The downcore record from this lake spans ca. 1-22 m. *Lake*
693 *Bourget* is a mesotrophic lake located in front of the French Alps (42 km², 146 m deep,
694 Jacob et al., 2008). The catchment area is characterized by a local river watershed of
695 600 km² and sporadic major flooding events of the Rhône River (Jacob et al., 2007).
696 The record covers a time span of ca. 3.5-9 ky BP. *Lake Van* is situated in eastern
697 Anatolia (Turkey) and is the world's largest soda lake (3570 km², 460 m deep, pH ~9.5-
698 9.9 and ~21-24 ‰ salinity; cf. Stockhecke, 2008). It receives water mainly through
699 precipitation and snowmelt from a catchment area estimated to be 12500 km² (cf.
700 Stockhecke, 2008). Seasonal traps were deployed between June 2006 and August 2007
701 deep in the lake, just above the sediments (Stockhecke, 2008).

702 **2. Marine samples**

703 **2.1. Water column, sediment trap, and surface sediments samples**

704 *Chipana Bay* is located off Northern Chile in one of the most productive areas of the
705 Humboldt Current system, characterized by cold upwelling bottom waters. The nearest
706 river (Loa River) has almost no outflow except during El Niño events, when the
707 discharge increases due to intense precipitation. The data set includes filtered water
708 samples taken at three depths in both February and August 2007 at ca. 1 km off Chipana
709 Bay. The depths were: 1) fluorescence maximum, 2) upper boundary of the oxycline,
710 and 3) 1 m above the seabed (ca. 90 m). The *Catalan Sea*, in the North Western
711 Mediterranean (Spain), is a comparatively productive area in the mostly oligotrophic

712 Mediterranean. The data set includes surface sediment (0-1 cm) obtained from transects
713 between the city of Barcelona and the Balearic Islands, i.e., from the southward directed
714 Catalan coastal current to the northward flowing modified Atlantic waters. The southern
715 *North Sea* is a shallow shelf sea (<50 m) characterized by a predominant influence of
716 coastal runoff. The surface sediment samples (0-1 cm) were taken in February, April,
717 and August at seven stations located within or at the outflow of the Dutch coastal
718 waters, characterized by high riverine freshwater input, and channel water of recent
719 oceanic origin (see Herfort et al., 2006 for more details on sample collection). One
720 station was located in the English coastal waters and East Anglian turbidity plume
721 (Herfort et al., 2006).

722 **2.2. Downcore records**

723 *Loch Sunart* is a marine fjord located in northwest Scotland. The loch is approximately
724 31 km long with an average width of 1.5 km. Peat bogs occur in the catchment. The
725 record spans an interval of 145 to 1745 cm, which correspond to approximately 465-
726 6637 ky BP. *Drammensfjord* is located in southern Norway and is a hyposaline (salinity
727 <32) silled basin with a length of 20 km and a width of 1.6–3 km. The Drammen River
728 feeds the Drammensfjord introducing a large volume of particulate matter and creating a
729 brackish surface layer on top of the saline bottom waters (Huguet et al., 2007). The
730 downcore record spans the most recent period, approximately the past 70 y (Huguet et
731 al., 2007). The *Amazon Fan* is the third largest submarine delta and is situated off the
732 northeastern coast of Brazil. The major input pathway in the Amazon Fan is from the
733 outflow of the Amazon River with a wide backland catchment area (Bendle et al.,
734 2010). Biomarkers of unambiguous terrestrial origin dominate the sediments (Bendle et
735 al., 2010 and references therein). The record used here spans approximately 13 m,
736 which correspond to the last 20 ky (Bendle et al. 2010).

737 The *Skagerrak* is a strait located between the North and the Baltic Sea (Scandinavia).
738 The water circulation in the Skagerrak is counterclockwise, with Atlantic water entering
739 along the Danish coast and Baltic water outflowing along the Norwegian coast. Most
740 suspended sediments entering the Skagerrak are supplied by large volumes of Atlantic
741 water. The Glomma River is the largest river draining into the Skagerrak and enters the
742 sea close to the coring site (cf. Rueda et al., 2009). The data included in this study cover
743 approximately the past 2000 y (see Rueda et al., 2009 for past 200 ky). *Guaymas Basin*,
744 located in the central Gulf of California (Mexico), has high productivity and low-
745 oxygen bottom waters. It is influenced by North Pacific deep and intermediate water as
746 well as subequatorial subsurface and equatorial surface water. Nutrients are brought to
747 the surface by tidal mixing around the islands north of Guaymas Basin and wind-driven
748 upwelling, fuelling high phytoplankton productivity (Cheshire et al., 2005 and
749 references therein). The record used here spans the upper 38 m (McClymont et al., in
750 press).

751 The *Alaskan coast* site (Gulf of Esquibel, USA) is located in an area of coastal
752 downwelling which, however, supports relatively high marine productivity. The site is
753 in inland waters adjacent to heavily forested, steep terrains that are presently glaciated
754 only in upland regions (Walinsky et al., 2009). The Alaskan coast record here includes
755 five samples from five depth intervals of a gravity core (5, 50, 80, 120, 140 cm depth).

756 The *Fram Strait* is the passageway between Greenland and Svalbard through which
757 warm saline waters are transported northwards with the West Spitsbergen Current (the
758 end member of the North Atlantic Current) and fresh water and sea ice is exported
759 southwards with the East Greenland Current. This record was retrieved from the
760 western continental margin of Svalbard and spans the last ~2000 years (Spielhagen et
761 al., 2011). Most of the recent organic matter is autochthonous with terrestrial organic

762 matter supply being likely the result of long range sea-ice transport from the north, with
763 contributions of the nearby Svalbard landmass (Birgel et al., 2004). The *NE Atlantic* site
764 is located in the northwestern flank of the Porcupine Seabight. The site is situated close
765 to a principal outlet glacier draining the British Ice Sheet and also receives ice rafted
766 debris derived from other North Atlantic margins (Peck et al., 2006). The record
767 comprises a sedimentary sequence with a time span of 15-25 ky, including two periods
768 of massive ice rafted debris input (Heinrich events; cf. Peck et al., 2006).

769 The *equatorial Pacific* site is located east of Galapagos Islands and is influenced by
770 the westwards flowing Southern Equatorial and the Peru Current Systems, including the
771 Humboldt Current. Sediments in this region very likely contain particles from both
772 windborne dust, transported by the southerlies, and submarine volcanic debris (Saukel
773 et al., 2011). The coring site possibly contained some fluvial debris originating from the
774 Gulf of Guayaquil on the eastern end of the Carnegie Ridge (Saukel et al., 2011). The
775 record spans the upper 1.4 m. The *equatorial Atlantic* record is located in the open
776 ocean within the southeastern margin of the Sierra Leone Rise. The region is
777 characterized by excellent preservation of the calcareous organisms, high sedimentation
778 rates, as well as windblown and fluvial delivery of diverse indicators of continental
779 climate (Shipboard Scientific Party, 1988). The record comprises a time span of ca. 0.96
780 – 1.12 million y BP. The *Benguela current* site is located off the West African coast,
781 where cold, nutrient-rich waters from the coastal upwelling area mix with low-
782 productivity oceanic water and form a zone of intermediate productivity (Shipboard
783 Scientific Party, 1998). The studied record covers approximately 340 m (ca. 2 million y
784 BP). The *subantarctic Atlantic* site is located in the open ocean within the present day
785 Subantarctic Zone (Martínez-García et al., 2009, 2011). It is characterized by relatively
786 low phytoplankton export production during interglacial periods and high export

787 production during glacial stages essentially stimulated by atmospheric supply of iron
788 (Martínez-García et al., 2009, 2011). The studied record covers a time span from the
789 mid-Pleistocene to the Holocene, encompassing several glacial and interglacial cycles
790 (MIS 1 to MIS 12, ca. 500 ky BP; Martínez-García et al., 2009).

791

792 **Appendix 1 References**

- 793 Bendle, J.A., Weijers, J.W.H., Maslin, M.A., Sinninghe, Damsté J.S., Schouten, S.,
794 Hopmans, E.C., Boot, C.S. and Pancost, R.D., 2010. Major changes in glacial and
795 Holocene terrestrial temperatures and sources of organic carbon recorded in the
796 Amazon fan by tetraether lipids. *Geochem. Geophys. Geosyst.* 11, Q12007,
797 doi:10.1029/2010GC003308
- 798 Birgel, D., Stein, R., Hefter, J., 2004. Aliphatic lipids in recent sediments of the Fram
799 Strait/Yermak Plateau (Arctic Ocean): Composition, sources and transport processes.
800 *Mar. Chem.* 88, 127-160.
- 801 Cheshire, H., Thurow, J., Nederbragt, A.J., 2005. Late Quaternary climate change
802 record from two long sediment cores from Guaymas Basin, Gulf of California. *J.*
803 *Quaternary Sci.* 20, 457–469.
- 804 Fietz, S., M. Sturm, Nicklisch A., 2005. Flux of lipophilic photosynthetic pigments to
805 the surface sediments of Lake Baikal. *Global Planet. Change* 46, 29-44.
- 806 Fietz, S., Nicklisch, A., Oberhänsli, H., 2007. Phytoplankton response to climate
807 changes in Lake Baikal during the Holocene and Kazantsevo Interglacials assessed
808 from sedimentary pigments. *J. Paleolimn.* 37, 177-203.
- 809 Henriksen, M., Mangerud, J., Matiouchkov, A., Murray, A.S., Paus, A., Svendsen, J.I.
810 2008. Intriguing climatic shifts in a 90 kyr old lake record from northern Russia.
811 *Boreas* 37, 20–37.
- 812 Herfort, L., Schouten, S., Boon, J.P., Wolering, M., Baas, M., Weijers, J.M.H., and
813 Sinninghe Damsté, J.S., 2006. Characterization of transport and deposition of
814 terrestrial organic matter in the southern North Sea using the BIT index. *Limnol.*
815 *Oceanogr.* 51, 2196–2205.
- 816 Huguet, C., Smittenberg, R.H., Boer, W., Sinninghe Damsté, J.S., and Schouten, S.
817 2007. Twentieth century proxy records of temperature and soil organic matter input in
818 the Drammensfjord, southern Norway. *Org. Geochem.* 38, 1838-1849.
- 819 Jacob, J., Disnar, J.-R., Arnaud, F., Chapron, E., Debret, M., Lallier-Vergès, E.,
820 Desmet, M., Revel-Rolland, M., 2008. Millet cultivation history in the French Alps as
821 evidenced by a sedimentary molecule. *J. Archaeol. Sci.* 35, 814-820.
- 822 Karabanov, E.B., Prokopenko, A.A., Williams, D.F., Khursevich, G.K., 2000. A new
823 record of Holocene climate change from the bottom sediments of Lake Baikal.
824 *Palaeogeogr. Palaeoclimatol.* 156, 211–224.
- 825 Kozhov, O.M., Izmet'eva, L.R., 1998. *Lake Baikal, Evolution and Biodiversity.*
826 Backhuys Publishers, Leiden.
- 827 Martínez-García, A., Rosell-Melé, A., Geibert, W., Gersonde, R., Masqué, P., Gaspari,
828 V., Barbante, C., 2009. Links between iron supply, marine productivity, sea surface
829 temperatures and CO₂ over the last 1.1My. *Paleoceanography*, PA1207. DOI:
830 10.1029/2008PA001657

831 Martínez-García, A., Rosell-Melé, A., Jaccard, S.L., Geibert, W., Sigman, D.M., Haug,
832 G.H., 2011. Southern Ocean dust-climate coupling during the past 4 million years.
833 Nature. doi: 10.1038/nature10310.

834 McClymont E.L., Ganeshram R., Pichevin L.E., Talbot H.M., van Dongen B.E.,
835 Thunell R.C., Haywood A.M., Singarayer J.S., Valdes P.J., *in press*. Sea-surface
836 temperature records of Termination 1 in the Gulf of California: challenges for
837 seasonal and inter-annual analogues of tropical Pacific climate change
838 (2011PA002226).

839 Müller, B., Maerki, M., Schmid, M., Vologina, E., Wehrli, B., Wüest, A., Sturm, M.,
840 2005. Internal carbon and nutrient cycling in Lake Baikal: sedimentation, upwelling
841 and early diagenesis. *Global Planet. Change* 46, 101-124.

842 Oberhänsli, H., Mackay, A.W., 2005. Introduction to ‘Progress towards reconstructing
843 past climate in Central Eurasia, with special emphasis on Lake Baikal’. *Global Planet.*
844 *Change* 46, 1-7.

845 Peck, V. L., Hall, I., Zahn, R., Elderfield, H., Grousset, F., Hemming, S.R., Scourse,
846 J.D., 2006. High resolution evidence for linkages between NW European ice sheet
847 instability and Atlantic Meridional Overturning Circulation. *Earth Planet. Sc. Lett.*
848 243, 476-488.

849 Rueda, G., Rosell-Melé, A., Escala, M., Gyllencreutz, R., Backman, J., 2009.
850 Comparison of instrumental and GDGT based estimates of sea surface and air
851 temperatures from the Skagerrak. *Org. Geochem.* 40, 287-291.

852 Rueda, G., Fietz, S., Rosell-Melé, A., (subm.). Coupling of Air and Sea Temperatures in
853 the Fram Strait during the Last 2000 Years. *Geophys. Res. Lett.*

854 Saukel, C., Lamy, F., Stuut, J.-B., Tiedemann, R., Vogt, C., 2011. Distribution and
855 provenance of wind-blown SE Pacific surface sediments. *Mar. Geol.* 280, 130-142.

856 Shipboard Scientific Party, 1988. Introduction and explanatory notes. In: Ruddiman W.,
857 Sarnthein M., Baldauf J., et al. (Eds.) *Proc. ODP, Init. Repts.*, 108: College Station, TX
858 (Ocean Drilling Program). doi:10.2973/odp.proc.ir.108.101.1988

859 Shipboard Scientific Party, 1998. Site 1084. In: Wefer, G., Berger, W.H., Richter, C., et
860 al., 1998. *Proc. ODP, Init. Repts.*, 175: College Station, TX (Ocean Drilling Program).
861 doi:10.2973/odp.proc.ir.175.1998

862 Spielhagen, R.F., Werner, K., Aagaard Sørensen, S., Zamelczyk, K., Kandiano, E.,
863 Budeus, G., Husum, K., Marchitto, T.M., Hald, M., 2011. Enhanced Modern Heat
864 Transfer to the Arctic by Warm Atlantic Water. *Science* 331, 450-453.

865 Stockhecke, M., 2008. The annual particle cycle of Lake Van: Insights from space,
866 sediments and water column. M.S. thesis. University of Zurich.

867 Walinsky, S.E., Prahl, F.G., Mix, A.C., Finney, B.P., 2009. Distribution and
868 composition of organic matter in coastal southeast Alaskan surface sediments. *Cont.*
869 *Shelf Res.* 29, 1565-1579.